STRUCTURAL
BIOLOGY

Volume 78 (2022)

Supporting information for article:

Radiation-induced defects in protein crystals observed by X-ray topography

Ryo Suzuki, Seiki Baba, Nobuhiro Mizuno, Kazuya Hasegawa, Haruhiko Koizumi, Kenichi Kojima, Takashi Kumasaka and Masaru Tachibana

S1. Irradiation effects observed by an optical microscope

In this article, we present four typical results. The glucose isomerase (GI) crystals are referred to as GI-01, GI-02, GI-03, and GI-04 crystals as shown in Figs. 1 and S1. For irradiation experiments, GI crystals were irradiated using focused X-ray beams with a size of 23×36 μm^2 at BL41XU in SPring-8, which were parallel to the [1 0 4] and [0 0 1] directions for the GI-01 crystal and [0 1 4] and [0 0 1] directions for the GI-02 crystal (the beam irradiated the crystal with a 30° tilt in the left region and a 45° tilt in the right region). The irradiation time was 1 s for each irradiation. Calculated values of the absorbed doses were 33.0 and 31.6 kGy for the GI-01 and GI-02 crystals, respectively. There were no noticeable contrasts in the crystal before irradiation, while two contrasts with spot shapes corresponding to the size of the focused X-ray beam appeared following irradiation (Fig. S2). This might be due to the solarization effect of the glass attached to the crystal holder, which is the change of the color due to the electron energy from the effect of radiation (Otley, 1952). The transparent color was changed to a slightly brownish one. Except for the discoloration of the glass, at this stage, there appeared to be no significant changes in the crystals observed using an optical microscope.

S2. Irradiation effects with different dose rates

The irradiation experiments were also performed using different absorbed doses at BL41XU in SPring-8. Four areas on the (101) plane of the GI-03 crystal were irradiated using a focused X-ray beam almost perpendicular to the plane (Fig. S3). Each irradiation was 1 s. Calculated values of the absorbed doses were 283, 55.1, 28.2, and 5.7 kGy for each irradiation. After irradiation, an optical micrograph was taken immediately (Fig. S3*d)*. At this stage, only the area irradiated with the high absorbed dose of 283 kGy exhibited some contrast, while in the optical micrograph, no significant change was observed in the other areas irradiated with the low absorbed doses of 55.1, 28.2, and 5.7 kGy (Fig. S3*d)*. Interestingly, the color of the area irradiated at 55.1 kGy, in addition to 283 kGy, changed 3 d after the irradiation (Fig. S3*e)*. After 136 d, the color of the area irradiated at 28.2 kGy also changed (Fig. S3*f*). The change in the color of the irradiated areas corresponds to etch pits of the dislocations, which may be due to the dissolving of the crystals or slight evaporation of intra-crystalline water, although the crystal holder was covered with a plastic slide using glue. Similar etch pits of the grown-in dislocations in GI crystals were observed (Koizumi *et al*., 2014; Suzuki *et al*., 2017). The dark contrasts with line shapes were elongated along the irradiated paths (Fig. S3*g–i)*. Moreover, some line contrasts were observed individually. The line contrasts appeared to elongate further with time, from both sides of the surface and bottom of the crystal toward the inside along the irradiated paths. These results suggest that the line contrasts in the optical micrographs may correspond to dislocation etch pits.

S3. Analysis of the introduction of dislocations based on the dislocation theory

According to dislocation theory (Hirth & Lothe, 1982; Hull & Bacon, 2011), the elasticity expression for the self-energy of dislocation is given by:

$$E=\frac{\mu b^2}{4\pi}\ln\frac{R}{r_0}$$

where μ is the shear modulus, b is the magnitude of Burgers vector, R is the crystal size, and r_0 is the size of dislocation core ($r_0 \sim 5b$). The energy is estimated using values of the shear modulus and Poisson's ratio, obtained from measurements of the sound velocities in T-HEWL crystals, as reported previously (Koizumi *et al*., 2009). Here, it was assumed that the values for GI crystals were similar to those for T-HEWL crystals. For easy estimation of energy, the crystal size was assumed as 1 mm. For GI-03, the estimated value of the dislocation energy with a Burgers vector of [1 0 1] was 1.7×10^{-7} J, which was lower than that of the dose, 5.7 kGy (= 5.3×10^{-6} J) with 1 s exposure. Similarly, the estimated value of the dislocation energy for T-HEWL was 1.1×10^{-7} J. This value was also lower than the dose, 9.6 kGy (= 1.2×10^{-6} J). However, in the case of GI-04, the estimated values of the dislocation energy with Burgers vector of [1 0 4], [5 4 5], and [6 5 18] were 1.8×10^{-6}, 4.7×10^{-6}, and 2.6×10^{-5} J, respectively. Although these values were comparable or higher than the dose of 1.5 kGy (= 1.3×10^{-6} J) with 1 s exposure, these were lower than the total dose of 222 kGy (= 1.9×10^{-4} J) with a 150 s exposure. This indicates that penetrating dislocations can be introduced using irradiation when the magnitude of the dose per 1 s exposure (dose rate) overcomes that of the self-energy of dislocation loops. The dose distribution for GI-03 and GI-04 is shown in Fig. S4. Simulation was carried out with cuboid crystals corresponding to the actual crystal size using RADDOSE-3D program (Zeldin *et al*., 2013) and R (www.r-project.org). None of the dose levels induced dislocations in GI-04.

S4. Irradiation of hen egg-white lysozyme crystals

Irradiation via a focused X-ray beam at BL41XU was also carried out for tetragonal hen egg-white lysozyme (T-HEWL) crystals. The irradiation time was 1 s. Dislocations were induced by irradiation, as in the cases of the GI crystals (Fig. S5). The calculated value of the absorbed dose was 9.6 kGy/s for the T-HEWL crystal. Moreover, the identified Burgers vectors corresponded to the irradiation direction, as in the cases of the GI crystals.

Table S1 Experimental conditions used for X-ray topography.

Sample No.	GI-01	GI-01	GI-02	GI-03	GI-03	GI-04
Thickness [μm]	540	540	860	970	970	1050
Facility	SPring-8	KEK-PF	SPring-8	SPring-8	KEK-PF	SPring-8
Beamline	BL38B1	BL14B	BL38B1	BL38B1	BL20B	BL38B1
Wavelength [Å]	1.3	1.2	1.3	1.2	1.2	1.2
Photon Flux [photons/s]	9.3×10^{10}	1.0×10^{11}	9.3×10^{10}	9.3×10^{10}	1.0×10^{11}	9.3×10^{10}
Beam size (H×V, FWHM)	4×4 mm^2	3×5 mm^2	4×4 mm^2	4×4 mm^2	3×5 mm^2	4×4 mm^2
Beam shape	Square	Rectangle	Square	Square	Rectangle	Square
Flux density [photons/mm^2/s]	5.8×10^{9}	6.7×10^{9}	5.8×10^{9}	5.8×10^{9}	6.7×10^{9}	5.8×10^{9}
Exposure time [s] (per one measurement)	180	180	180	180	180	180
Total dose [kGy]*	0.3	0.3	0.2	0.2	0.2	0.2

*The dose was calculated including the attenuation effect of the cover glass since the incident X-ray entered to the crystal through the glass. The transmittance of X-ray for the cover glass used in this experiment condition is approximately 0.55. In this study, the average dose on the exposed region was used.

Table S2 Experimental conditions used for X-ray irradiation.

Sample No.	GI-01	GI-02	GI-03	GI-04
Thickness [μm]	540	860	970	1050
Beamline	BL41XU	BL41XU	BL41XU	BL38B1
Wavelength [Å]	1.0	1.0	1.0	1.0
Photon Flux [photons/s]	1.3×10^{13}	1.3×10^{13}	1.3×10^{13}	7.5×10^{9}
Beam profile*	Top hat	Top hat	Top hat	Gaussian
Beam size (H×V, FWHM)	22×37 μm^2	22×37 μm^2	22×37 μm^2	36×30 μm^2
Beam shape	Rectangle	Rectangle	Rectangle	Circle (Pinhole)
Flux density [photons/mm^2/s]	1.6×10^{16}	1.6×10^{16}	1.6×10^{16}	8.3×10^{12}
Exposure time [s]	1	1	1	150
Attenuation factor**	0.0100	0.0100	0.0959 0.0187 0.00958 0.00193	1
Dose rate [kGy/s]***	33.0	31.6	283 55.1 28.2 5.7	1.5
Total dose [kGy]***	33.0	31.6	283 55.1 28.2 5.7	222
Incident direction	[1 0 4] [0 0 1]	[0 1 4] [0 0 1]	[1 0 1]	[1 0 4] [6 5 18] [5 4 5]
Burgers vector ***b***	–	0 0 1	1 0 1	–

*The dose was calculated with assuming the beam profile as top hat for BL41XU, and Gaussian for BL38B1. **Various Aluminium plates were used as attenuator. For GI-04, there was no attenuator. ***The dose was calculated including the attenuation effect of the cover glass since the incident X-ray entered to the crystal through the glass. The transmittance of X-ray for the cover glass used in this experiment condition is approximately 0.55. In this study, the average dose on the exposed region was used. It is noted that all

calculation of the absorbed dose was carried out using the actual crystal thickness, which was measured by the observation in an optical microscope, and the beam size.

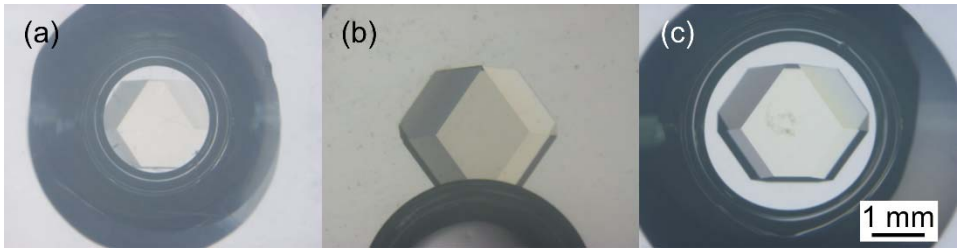

Figure S1 Optical micrographs for (*a*) GI-02, (*b*) GI-03, and (*c*) GI-04 crystals.

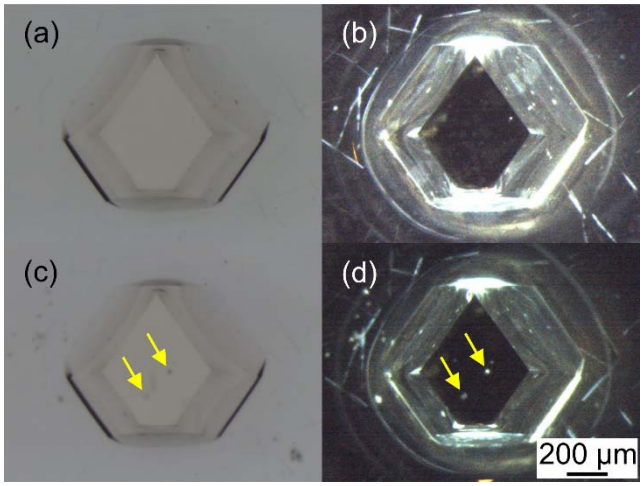

Figure S2 Optical micrographs of GI-01 crystal. (*a*, *c*) Bright-field and (*b*, *d*) dark-field micrographs before and after irradiation, respectively. The arrows in (*c*) and (*d*) correspond to the irradiation sites.

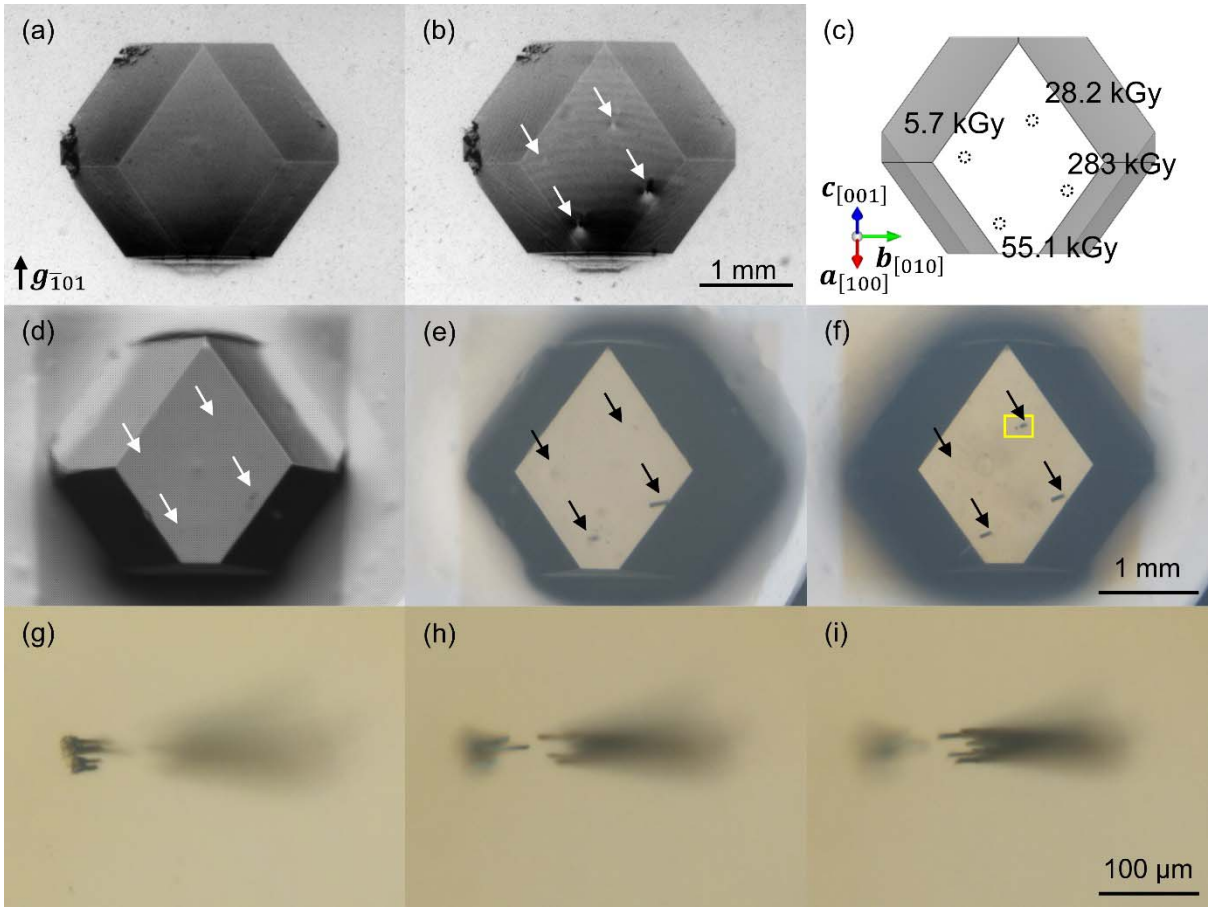

Figure S3 (*a*, *b*) X-ray topographs for GI-03 crystal taken with $\bar{1}01$ diffraction before and after irradiation, respectively, and (*c*) the corresponding schematic. (*d*–*f*) Optical micrographs taken 3 and 136 d after irradiation, respectively. The arrows in (*b*), (*d*), (*e*), and (*f*) correspond to irradiation sites. (*g*–*i*) Extended figures of the surface side, inside, and glass side of the crystal, respectively, indicated by the yellow square in (*f*).

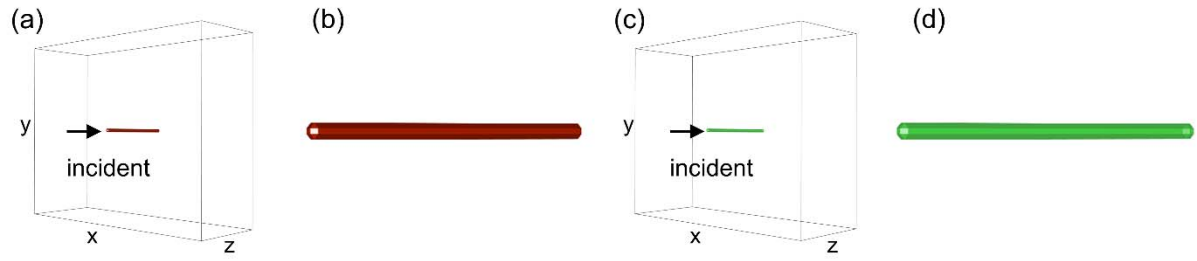

Figure S4 Dose distribution for (*a*, *b*) GI-03 and (*c*, *d*) GI-04, respectively modelled in RADDOSE-3D (Zeldin *et al*., 2013) and R (www.r-project.org). (*b*) and (*d*) present the magnified views of the dose area with the same direction as in (*a*) and (*d*), respectively. Note that the lengths of *x*, *y*, and *z* corresponding to the crystal size are 2.9, 2.3, and 0.97 mm for GI-03, and 2.9, 2.3, and 1.05 mm for GI-04, respectively. Each crystal size was measured by optical microscope observation. The red and green colors correspond to dose levels higher and lower than the dislocation energy, respectively. In (*a*), the dose levels overcame the dislocation energy. In (*b*), there was no dose level to induce dislocations. The dose distribution was uniform for each path.

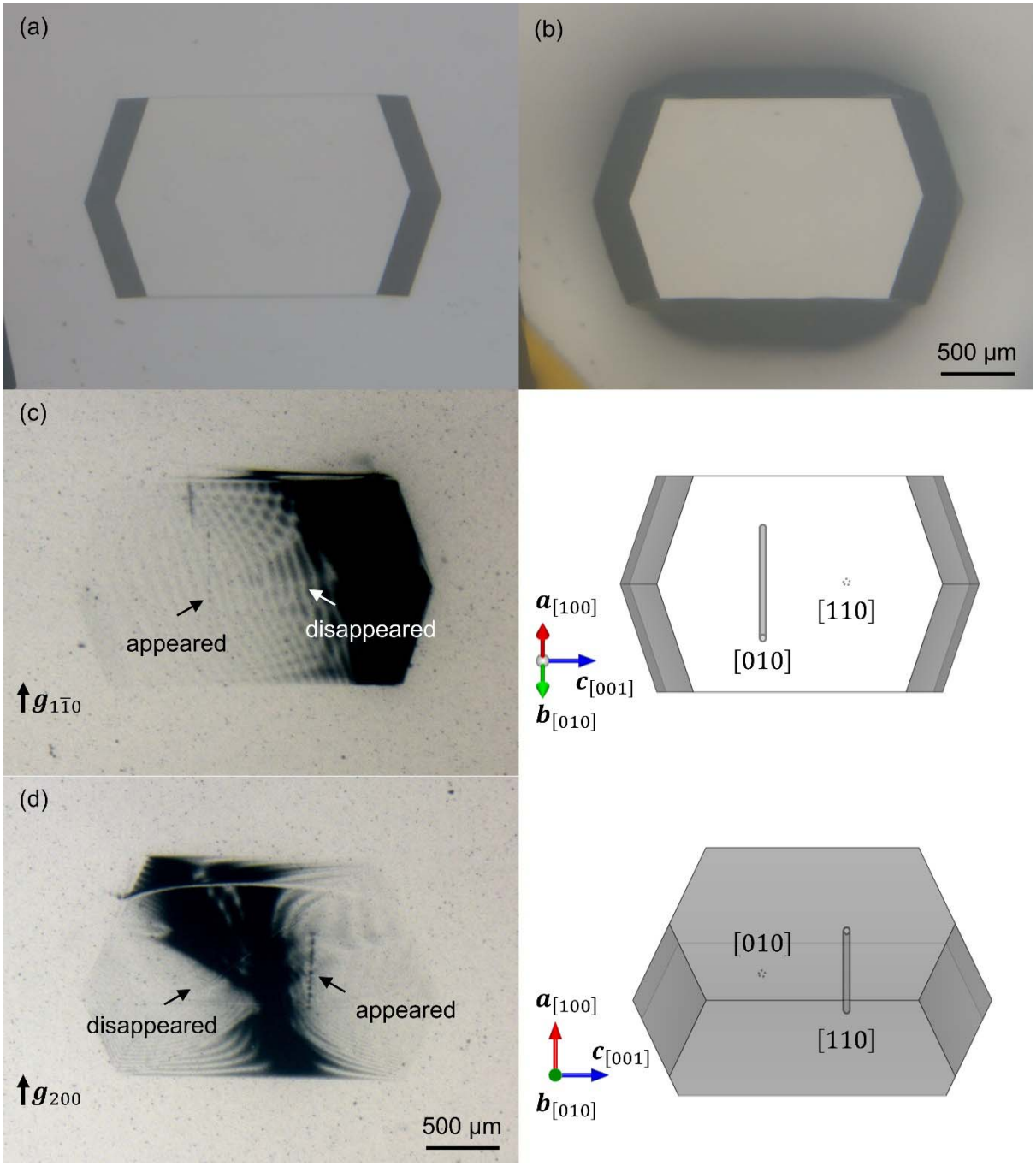

Figure S5 (*a*, *b*) Optical micrographs of the hen egg-white lysozyme crystal before and after irradiation, respectively. X-ray topographs taken with (*c*) $1\,\bar{1}0$ diffraction and (*d*) 200 diffraction after irradiation. Figures (*c*) and (*d*) on the right correspond to the schematics. The columns correspond to the irradiation paths. Note that the visibility of contrasts depends on the diffraction vector. The line contrasts corresponding to the irradiation disappear in (*c*) and (*d*).

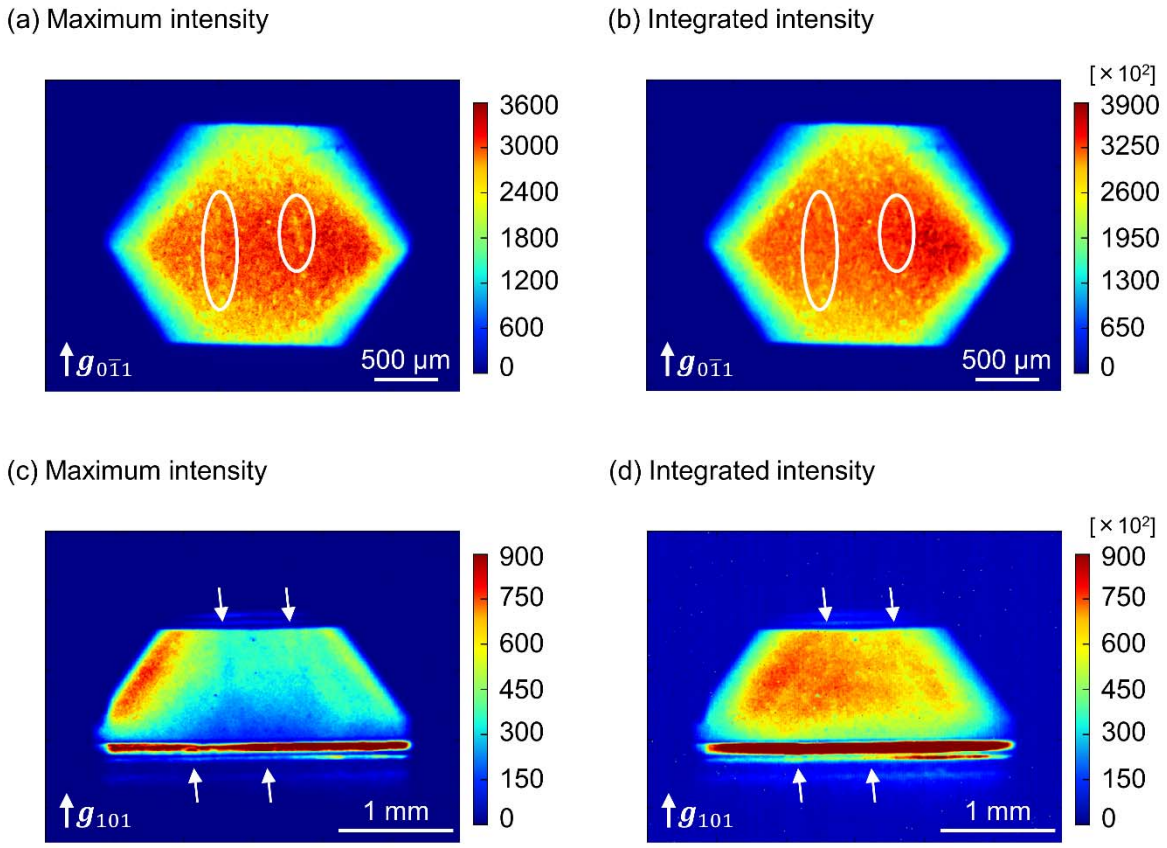

Figure S6 The map of (*a*, *c*) maximum intensity and (*b*, *d*) integrated intensity for GI-02 and GI-03, respectively. White circles and arrows show dislocation areas (corresponding to dislocations shown in Figs. 2*a* and 3*a*).